Structural Dynamics of Transfer Ribonucleic Acid: Carbon-13 Nuclear Magnetic Resonance of [^{13}C]Methyl-Enriched Pure Species†

Randall A. Kopper, Paul G. Schmidt, and Paul F. Agris*

ABSTRACT: Carbon-13 nuclear magnetic resonance (NMR) of ^{13}C-enriched methyl groups native to tRNA has been used to investigate the structure and dynamics of four purified species of *Escherichia coli* tRNA. All four tRNA species, Phe, Cys, Tyr, and Ser-1, exhibited resonances from the hypermodified nucleoside 2-(methylthio)-N^6-(Δ^2-isopentenyl)-adenosine (ms^2i^6A) and from ribothymidine (T). In addition, $tRNA^{Phe}$ yielded a peak for 7-methylguanosine; $tRNA^{Tyr}$ and $tRNA^{Ser}$, resonances for 2′-*O*-methylguanosine; and $tRNA^{Ser}$ for 2′-*O*-methylcytidine (Cm). Carbon-13 enrichment was restricted to the methyl groups, which were approximately 70 atom % ^{13}C, resulting in site-specific ^{13}C NMR probes in the TψCG, dihydrouridine, and anticodon loops of tRNA. Multiple peaks for the methyl groups of T in $tRNA^{Phe}$ and $tRNA^{Tyr}$ and Gm in the latter indicated multiple structural forms for the regions of the molecule probed. These multiple forms coalesced to a single structure upon the addition of $MgCl_2$. In contrast, tRNAs specific for Cys and Ser existed in only one major structural form in both the absence and presence of Mg^{2+}. Transfer RNAs specific for Phe and Tyr exhibited a single peak for T in the absence of Mg^{2+} after thermal denaturation (at approximately 36 °C) downfield of that for tRNA in the presence of Mg^{2+}. In the presence of Mg^{2+}, the chemical shift of the T methyl group in $tRNA^{Phe}$ and $tRNA^{Cys}$ was 11.20 ppm, whereas, in $tRNA^{Ser}$ and $tRNA^{Tyr}$, it was 11.10, suggesting that different structural environments may exist in portions of different tRNAs in their native states. Values of spin–lattice relaxation times, nuclear Overhauser enhancements (NOE), and line widths for the methyl carbons of tRNA in the presence of Mg^{2+} at 25 °C were utilized for determining rotational reorientation correlation times. The different tRNA species had significantly different apparent overall rotational correlation times (τ_R). Transfer RNA^{Phe} reoriented most rapidly with τ_R of 12 ns, whereas $tRNA^{Cys}$ was approximately twice this reorientation time. Since the two molecules are about the same in molecular weight, τ_R may reflect true differences in the motional capabilities of large sections of the two tRNA structures. Internal correlation times for diffusion of the methyl group on its axis varied between 0.4 and 1.6 ps for the methyl of T and 0.8 and 2.0 ps for the methylthio of ms^2i^6A for the four tRNA species. The 2′-*O*-methyl resonance of $tRNA^{Ser}$, having a chemical shift of 58.36 ppm and tentatively assigned to Cm in the anticodon loop, exhibited a remarkably large NOE, 2.3, and a large T_1, 2.0 s. This suggests that the methyl carbon experiences motion of the C_2–O bond in addition to simple methyl rotation. However, for the majority of the methyl groups fast diffusional reorientation about the methyl–base or methyl–S bond was the greatest contributor to relaxation from internal motion. Enough differences in tRNA spectra, relaxation rates, NOE, and calculated τ_R and τ_i values exist among the four tRNA species to conclude that there are differences in structure and dynamics, especially in the region of the TψCG loop interaction with the dihydrouridine loop.

The modified nucleosides of transfer RNA molecules are found consistently located at specific positions in the nucleoside sequence and secondary structure of the almost 200 tRNAs studied (Agris, 1983; Dirheimer et al., 1979; Sprinzl & Gauss, 1982). Methylated nucleosides—such as m^5U(T) in the T loop, m^7G in the extra arm, ms^2i^6A or other hypermodified purines adjacent to the third nucleoside of the anticodon, and Gm in the D loop—are particularly known for this consistency of position. Therefore, if methyl groups could be used as probes of the native tRNA structure, they may be useful in distinguishing tertiary structures of tRNA species having differences in sequence but otherwise identically positioned methylated nucleosides. These probes may also be sensitive to the structural dynamics of the molecule in solution.

We have been able to ^{13}C enrich exclusively and to a high degree the methyl carbons of the methylated nucleosides occurring naturally in *Escherichia coli* tRNA (Tompson et al., 1979; Tompson & Agris, 1979). Thus, the [^{13}C]methyls become ^{13}C NMR[1] probes of structure. Our initial NMR analyses of unfractionated tRNA (Tompson et al., 1979) and preliminary studies of three purified species that exhibited single-carbon resonance resolution (Agris & Schmidt, 1980) indicated that chemical shifts of the methyl groups indeed were sensitive to structure and structural perturbations.

Insights into rates and amplitudes of internal motion have been gained from analysis of ^{13}C NMR relaxation times (T_1 and T_2) and the nuclear Overhauser effect for methyl groups in proteins (London, 1980). Therefore, we thought that similar measurements in tRNA might reflect structural arrangements in close proximity to the methyl groups of a nucleic acid. The results show that relaxation times are sensitive probes of local structure in tRNA.

Materials and Methods

Materials. [^{13}C]Methyl-L-methionine (90+ atom %) was purchased from Merck and Co., Inc., Montreal, Canada. Carbon-13-enriched tRNAs were isolated from *Escherichia coli* C6 rel$^-$met$^-$cys$^-$ strain M1. Unlabeled *E. coli* B tRNA was obtained directly from Plenum Scientific Research, Inc., Hackensack, NJ. D_2O (99.9 atom %) was supplied by Aldrich Chemical Co. All other chemicals were of reagent-grade purity.

^{13}C Enrichment of tRNA. *E. coli* C6 rel$^-$met$^-$cys$^-$ strain

† From the Division of Biological Sciences, University of Missouri, Columbia, Missouri 65211 (R.A.K. and P.F.A.), and the Oklahoma Medical Research Foundation and the Department of Biochemistry and Molecular Biology, University of Oklahoma Health Sciences Center, Oklahoma City, Oklahoma 73104 (P.G.S.). *Received August 2, 1982.* This research was financially supported by Research Grants GM23037 from the National Institutes of Health to P.F.A. and GM25261 to P.G.S. P.G.S. acknowledges receipt of a Research Career Development Award (AM00525) and P.F.A. acknowledges receipt of a National Research Service Award Senior Fellowship (F33-GM07826), both from the National Institutes of Health.

[1] Abbreviations: NMR, nuclear magnetic resonance; DEAE, diethylaminoethyl; NOE, nuclear Overhauser effect; FID, free-induction decay.

0006-2960/83/0422-1396$01.50/0

M1 was grown in 15-L batches at 37 °C in stringently defined minimal media containing [^{13}C]methyl-L-methionine (Tompson & Agris, 1979). Cells were harvested in late log phase and nucleic acids isolated by extraction with phenol (Agris et al., 1973a,b). Carbon-13-enriched tRNA was obtained by DEAE-cellulose chromatography of the unfractionated nucleic acids. The ^{13}C enrichment, determined from ^{13}C NMR spectra of the tRNA without NOE, was better than 70 atom % and restricted to the methyl groups. Previous mass spectrometric studies of isolated nucleosides indicated approximately 60 atom % [^{13}C]methyl groups in the tRNA (Agris et al., 1980).

Purification of Individual tRNA Species. Both the ^{13}C-enriched and unlabeled tRNA were fractionated into pure species by sequential benzoylated DEAE-cellulose (BDC) and reversed-phase (RPC-5) column chromatography. Column fractions were monitored by UV absorbance at 260 nm and assayed for specific species by aminoacylation with radiolabeled amino acids by using unfractionated *E. coli* B aminoacyl-tRNA synthetase (Agris & Schmidt, 1980). The purity of the tRNA species obtained was determined by quantitative aminoacylation (Agris et al., 1973b; Seno et al., 1974) and polyacrylamide gel electrophoresis (Agris et al., 1974).

Transfer RNA samples were concentrated by ethanol precipitation, redissolved in water, and dialyzed extensively against glass-distilled water. Each sample was then evaporated under vacuum to near dryness and brought to the desired volume with D_2O. Samples for carbon NMR were placed in 0.25-mL Wilmad glass small-sample insert bulbs in a 10-mm tube containing H_2O. Proton NMR measurements were done with 0.5-mL samples in 5-mm NMR tubes.

NMR Measurements. NMR spectra at 75.5 MHz (^{13}C) or 300 MHz (^{1}H) were collected with a quadrature-detection Fourier-transform spectrometer composed of a CMS 70/50 magnet, a 10-mm carbon probe or a 5-mm proton probe (Cryomagnet Systems, Indianapolis, IN), a Nicolet 1180 computer, and in-house radio-frequency equipment. A Bruker unit maintained constant temperature while the actual sample temperature was measured with a thermocouple inserted into the H_2O around the microcell containing the sample. Carbon-13 T_1s were measured by the progressive saturation technique (Freeman & Hill, 1971) with 90° pulses of 20 μs. Relaxation times were taken from a least-squares fit of the data to an exponential. T_2 values were estimated from line widths after correction for inhomogeneity and digital broadening. NOE measurements utilized gated broad-band ^{1}H decoupling for the null measurements and continuous broad-band decoupling for expression of the NOE. In both cases, the computer cycled back and forth between sets of FIDs to maintain a relatively constant temperature. Delay times in the gated decoupling experiment were carefully checked to allow full relaxation of magnetization to its equilibrium level, making note of the observation that long ^{1}H T_1 values may dictate extended wait times (Jelinski et al., 1980). Normal proton NMR spectra were collected with a 90° pulse of 4.5 μs. Transverse relaxation rates were measured with the Hahn spin-echo pulse sequence (90–τ–180–τ), employing delays from 2–60 ms. Relaxation rates (T_2) were calculated with a programmed routine for fitting the function $y = A^{-x/T}$ to experimental data points where A is the y intercept at x equal to 0, T is T_2, and x is 2 times the delay in the Hahn spin-echo experiment. The best fit in this program is that which has a minimum χ^2.

Results and Discussion

Four [^{13}C]methyl-enriched transfer RNAs specific for Phe, Cys, Tyr, and Ser were chosen for study. The nucleoside sequences of these tRNAs are known (Sprinzl & Gauss, 1982), and the tRNAs constitute an interesting family since they all contain ms^2i^6A and recognize codons starting with uridine. Hydrophobicity of ms^2i^6A enabled purification of the four tRNAs to be accomplished relatively easily. The individual tRNA species were purified by sequential benzoylated DEAE-cellulose and RPC-5 column chromatography (see Materials and Methods). Most of the ^{13}C NMR data presented here were collected on $tRNA^{Phe}$ due to its high purity and the large yield from unfractionated tRNA (Agris & Schmidt, 1980). Transfer RNA^{Tyr} was found to contain a small amount of a single second species that was conclusively identified as $tRNA^{Trp}$ by its elution position during chromatography, aminoacylation, detection in urea–polyacrylamide gel electrophoresis, and the presence of signals from both m^7G and an additional 2′-*O*-methyl group in the NMR spectrum (Figure 1).

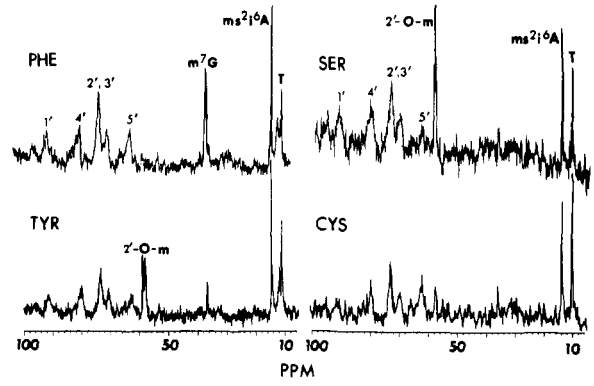

FIGURE 1: Carbon-13 NMR spectra of [^{13}C]methyl-enriched *E. coli* tRNA specific for Phe, Tyr, Ser, and Cys. Solutions of purified tRNA species, [^{13}C]methyl enriched in vivo, were prepared and placed in 0.25-mL microsample inserts for ^{13}C NMR as described under Materials and Methods. The samples were of the following approximate concentrations: $tRNA^{Phe}$, 2 mM; $tRNA^{Tyr}$, 1.8 mM; $tRNA^{Ser}$, 1.5 mM; $tRNA^{Cys}$, 1.2 mM. Proton-decoupled spectra (8096 points) were taken at 25 °C with a 60° pulse of 12 μs, 2.5-s delay, ±8000-Hz sweep width, and different numbers of acquisitions between 8000 and 16 000. Note the multiple resonances for the methyl of T in Phe and Tyr but not Ser and Cys.

^{13}C NMR Spectra. All ^{13}C NMR spectra were acquired with approximately 2 mM tRNA solutions. This concentration was made possible by the use of 0.25-mL glass small-sample insert bulbs (Wilmad) and required only 0.50 μmol of tRNA. Use of the 0.25-mL inserts made feasible the NOE and relaxation studies described below due to the increased signal to noise ratio not previously possible. The tubes containing these inserts were positioned very precisely within the magnetic field to optimize both the signal to noise ratio and line shapes. The 90° pulse width, 20 μs, was determined in both a dilute dioxane–ethylene glycol solution in D_2O and a 2 mM solution of $tRNA^{Phe}$ at 25 °C in the 0.25-mL inserts. For experiments in the presence and absence of magnesium and those involving temperature dependence, the chemical shifts of all ^{13}C signals were measured relative to that of ms^2i^6A, which was taken as a standard and assigned a value of 14.70 ppm. The methyl carbon signal from the methylthio group has been shown to be least affected by its environment (Tompson et al., 1979).

The position and degree of ^{13}C enrichment was determiend by comparison of the integrated peak areas of the NMR spectrum without nuclear Overhauser enhancement (NOE). Signal areas of the various methyl groups were compared with those of the natural abundance signals from the ribose carbons. For example, the integrated peak areas for a $tRNA^{Phe}$ spec-

Table I: [^{13}C]tRNA Chemical Shifts (ppm) at 25 °C

	Phe		Cys		Tyr		Ser	
carbon	with Mg	no Mg	with Mg	no Mg	with Mg	no Mg	with Mg	no Mg
1′	92.25	91.50		91.25	91.87	91.45	90.68	91.60
4′	80.30	80.44	84.36	79.92	80.24	80.39	79.86	80.34
2′, 3′	73.78	73.73	74.15	73.35	73.45	73.79	73.14	73.77
2′, 3′	70.72	70.83		70.79	69.85	70.80	69.85	70.38
5′	62.98	63.01	62.24	62.91	62.76	62.76	62.87	62.65
2′-OM					59.10	59.10	58.97	
					58.37	58.43	58.35	
						58.32		58.37
								57.85
m^{7}G	37.21	37.17						
		36.81						
ms[a]	14.70	14.70	14.70	14.70	14.70	14.70	14.70	14.70
		12.87						
		11.85				12.19		
						12.04		
T	11.20	11.24	11.20	11.20	11.10	11.20	11.10	11.20

[a] All values of ppm were normalized to ms at 14.7 ppm.

trum indicated that the 90+ atom % [^{13}C]methylmethionine precursor was incorporated into the methyl groups of tRNA^{Phe} with a dilution of the label to approximately 70 atom %.

Divalent Metal Ion and Temperature Dependence of Chemical Shifts. The spectra in Figure 1 illustrate that at 25 °C and in the absence of added magnesium, all of the tRNAs studied exhibited the appropriate methyl signals for Gm, Cm, m^{7}G, ms^{2}i^{6}A, and T as expected from the tRNA sequences. The tRNA^{Phe} and tRNA^{Tyr} spectra contain multiple ribothymidine peaks, in contrast to the tRNA^{Cys} and tRNA^{Ser} spectra, which contain sharp singlets for this nucleoside. In the case of tRNA^{Phe}, the multiple T signals collapse into a single upfield peak upon the addition of magnesium (see Figures 2 and 4 for comparison to Figure 1). A single downfield peak is obtained, as expected, when the tRNA structure is "melted" by raising the temperature. This observation confirms that reported earlier (Agris & Schmidt, 1980) but illustrates this phenomenon with a much higher signal to noise ratio. In addition, the same results have been obtained for tRNA^{Tyr}. Transfer tRNA^{Cys} and tRNA^{Ser} never exhibited multiple T signals at any temperature or magnesium concentration. In fact, no multiple signals from T were observed for any tRNA sample in the presence of magnesium at any temperature.

The chemical shift of the T methyl signal at 11.20 ppm for tRNA^{Cys} was not affected by the addition of magnesium but moved upfield to 11.10 ppm in the case of Mg^{2+} addition to tRNA^{Ser} (Table I). All of the T signals of tRNA^{Phe} and tRNA^{Tyr} were shifted upfield from the forms present in the absence of magnesium, although by different extents to yield a single signal at 11.20 ppm for tRNA^{Phe} and at 11.10 for tRNA^{Tyr}. These results suggest the existence of two major classes of tRNAs: one in which T is maintained in a very similar environment in both the presence and absence of magnesium and another in which the tRNAs undergo a significant conformational change, at least in the vicinity of T, to assume a single native conformation upon the addition of magnesium. It is also of interest that in the presence of Mg^{2+}, tRNA^{Ser} and tRNA^{Tyr} signals for T have a chemical shift of 11.10 ppm, whereas the spectral position of the T signals in the other native tRNAs (in the presence of magnesium) is 11.20 ppm.

The spectra of tRNA^{Ser} and tRNA^{Tyr} (Figure 1) each exhibited two signals from 2′-*O*-methyls. The tRNA^{Ser} sequence contains a Gm at position 18 and a Cm at position 32. Transfer RNA^{Tyr} contains a Gm at position 18 but no Cm.

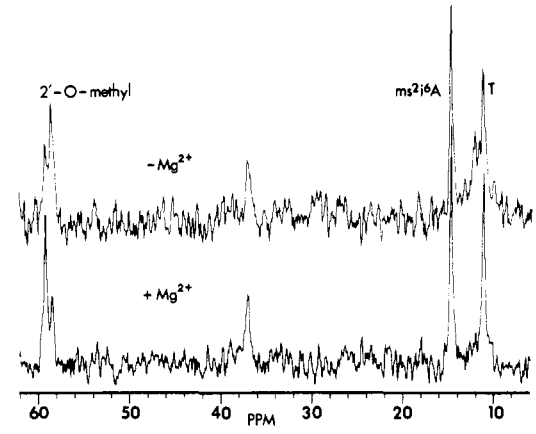

FIGURE 2: Effect of $MgCl_2$ on methyl carbon resonances of tRNA^{Tyr}. Spectra were taken of 1.8 mM tRNA^{Tyr} in the absence or presence of 10 mM $MgCl_2$. These spectra were taken at 25 °C with a 90° pulse, 8-s delay, and 2800 acquisitions and were processed with a digital line broadening of 10 Hz. With addition of $MgCl_2$, multiple forms of the T signal become one upfield resonance, and the majority of the 2′-*O*-methyl signal, Gm, moves downfield. The smaller signals at 37.2 and 58.4 ppm in the spectrum of the sample with Mg^{2+} are attributed to the m^{7}G and Cm, respectively, within the small amount of tRNA^{Trp} in the preparation.

However, our preparation of tRNA^{Tyr} is approximately 70% tRNA^{Tyr} and 30% tRNA^{Trp}, which does contain a Cm at position 32 but no Gm. In the presence of Mg^{2+}, both tRNAs Tyr and Ser exhibited a signal at 58.36 ± 0.01 ppm (Table I). In addition, tRNA^{Ser} had a 2′-*O*-methyl signal at 58.97 ppm and tRNA^{Tyr} had a resonance at 59.10 ppm. In the case of tRNA^{Tyr} and not tRNA^{Ser}, the addition of Mg^{2+} changed the relative signal strength of the two resonances, making the smaller downfield signal now the more prominent of the two (Figure 2). Therefore, we suspect that the methyl of Gm, like that of T, is probing multiple forms of this tRNA that conform to a single dominant structure in the presence of Mg^{2+}. With Mg^{2+} present, the downfield peak can be tentatively assigned to Gm and the small upfield resonance to the Cm of that small amount of tRNA^{Trp} within the Tyr preparation. Thus, the two 2′-*O*-methyl resonances of tRNA^{Ser} may be assigned to Gm (58.97 ppm) and Cm (58.36 ppm); however, in contrast to tRNA^{Tyr}, multiple conformations are not probes in tRNA^{Ser}. The chemical-shift difference between the two 2′-*O*-methyls in each of the tRNAs, 0.61 ppm for tRNA^{Ser} and 0.74 ppm for tRNA^{Tyr}, far exceeds the 0.1-ppm difference in chemical shifts for the mononucleosides: Gm, 59.00 ppm;

Table II: $tRNA^{Phe}$ ^{13}C Chemical Shifts (ppm): Temperature Dependence

	carbon		
temp (°C)	m^7G	ms	T
25	37.23	14.70	11.20
30	37.19	14.70	11.21
36	37.15	14.70	11.18
45	37.10	14.70	11.22
52	36.99	14.70	11.66
63	36.97	14.70	12.24

Cm, 58.90 ppm (P. F. Agris, unpublished results). Thus, chemical-shift differences in each of these tRNA preparations are due to something beyond simply the nature of the base to which the ribose is attached. Most likely, it is due to position within the tertiary structures of the molecules since both the Gm and Cm signals are coincident with that of the mononucleosides when tRNA is heat denatured.

Table II shows the effect of temperature on the chemical shifts of m^7G and T in $tRNA^{Phe}$ (10 mM $MgCl_2$). Significantly, the signal from m^7G moved progressively upfield as the molecule was melted. The T signal, however, moved in the expected downfield direction as the molecule became denatured. Major changes in the chemical environment around T appear to take place from 45 to 52 °C (Δppm = 0.44) and from 52 to 63 °C (Δppm = 0.58). The chemical shift of m^7G changed more gradually by only 0.24 ppm over the entire temperature range. The final high-temperature chemical shifts (Table II) for both modified nucleosides within the almost completely denatured tRNA structure corresponded closely to the values for the free nucleosides (Tompson et al., 1979).

NMR Relaxation Times and NOE Values. Spin–lattice relaxation times (T_1) were determined by progressive saturation. The T_1s of the ^{13}C-enriched methyl groups of the four different tRNAs, Phe, Cys, Tyr and Ser, were measured at 25 °C in the presence and absence of 10 mM $MgCl_2$ (Table IIIA). The range of values among the tRNA species for both

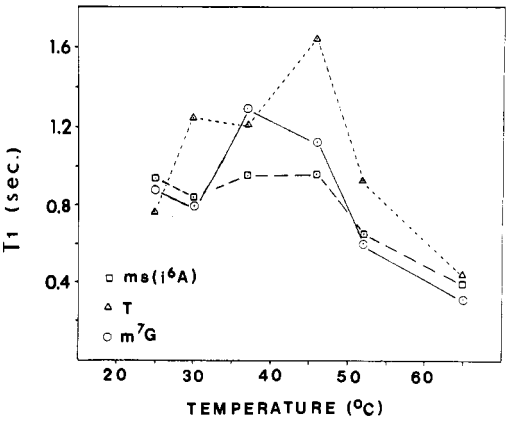

FIGURE 3: Temperature dependence of spin–lattice (T_1) relaxation of $tRNA^{Phe}$ methyl carbons. Transfer RNA^{Phe} at a concentration of approximately 1 mM with 10 mM $MgCl_2$ was subjected to thermal denaturation in a 0.25-mL microsample NMR insert. T_1 values for ^{13}C-enriched methyls were measured by progressive saturation at six temperatures (22, 30, 36, 46, 52, and 65 °C). For measurement of T_1 at each temperature, spectra were taken with a 90° pulse, 4800 accumulations from 22 to 46 °C and 3000 accumulations for 52 and 65 °C, and seven delays between 0.4 and 6 s. The figure shows a plot of T_1 vs. temperature for the methyls of T, ms^2i^6A, and m^7G.

T and ms^2i^6A was much smaller in the absence of Mg^{2+}, approximately 0.3 s, than with the addition of Mg^{2+}, approximately 1.3 s. Notably, all values *increased* with the addition of $MgCl_2$.

Temperature dependence of T_1 was studied for the ^{13}C-enriched methyl groups of $tRNA^{Phe}$ in the presence of 10 mM Mg^{2+} (Figure 3). The T_1 of the methyl carbon of ms^2i^6A increased only slightly between 24 and 46 °C and then dropped with the continued thermal denaturation of the tRNA molecule, as seen in Figure 3. The final T_1 for the denatured molecule at 65 °C was 0.4 s. Changes in T_1 with temperature for the methyl groups of T and m^7G were more interesting. For T, the value of T_1 increased in two steps, from 25 to 30

Table III

(A) Spin-Lattice Relaxation Times of tRNA Methyl Carbons [T_1 (s), 25 °C]

	2-OCH_3		m^7G		ms (i^6A)		T	
	with Mg	no Mg	with Mg	no Mg	with Mg	no Mg	with Mg	no Mg
Phe			0.94	0.78	0.94	0.73	0.76	0.74
Cys					2.10	0.74	1.67	0.98
Tyr	1.35, 2.08	0.88, ND[a]			1.29	1.08	1.86	1.03
Ser	1.15, 2.04	0.63, 0.69			1.06	0.97	1.14	1.02

(B) Nuclear Overhauser Enhancement (1 + η)

	2-OCH_3		m^7G		ms (i^6A)		T	
	with Mg	no Mg	with Mg	no Mg	with Mg	no Mg	with Mg	no Mg
				NOE at 25 °C				
Phe			1.43	1.62	1.69	1.55	1.53	2.08
Cys					1.66	1.54	1.28	1.79
Tyr	1.53, ND	1.63, 2.15			1.44	1.44	1.56	1.77
Ser	1.45, 2.30				1.44		1.30	
				NOE at 36 °C				
Phe				1.56		1.36		1.53
Cys						1.49		1.38

(C) Methyl Carbon Line Widths (Hz) at 25 °C

tRNA	length	2-OCH_3	m^7G	ms (i^6A)	T
Phe	76		15	8	10
Cys	74			14	12
Tyr	85	23		11	11
Ser	88	19, 27		7	14

[a] ND, not determined.

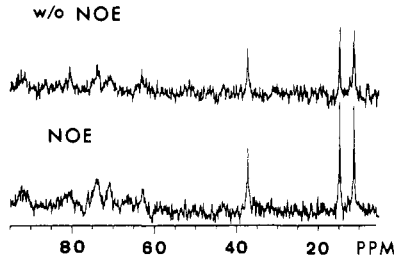

FIGURE 4: Nuclear Overhauser enhancement of methyl carbon signals from $tRNA^{Phe}$. Spectra of $tRNA^{Phe}$ (10 mM $MgCl_2$) were collected at 25 °C with and without nuclear Overhauser enhancement by cycling between the two data sets of continuous and gated proton decoupling in order to reduce any possible temperature differences. A pulse of 90° and a delay of 6 s were used in the collection of 4000 scans for each spectrum. Natural abundance (1.1%) ^{13}C resonances of the ribose carbons (between 50 and 90 ppm) are seen in the spectra, as well as the ^{13}C-enriched methyls of T (11.20 ppm), ms^2i^6A (14.70 ppm), and m^7G (31.21 ppm).

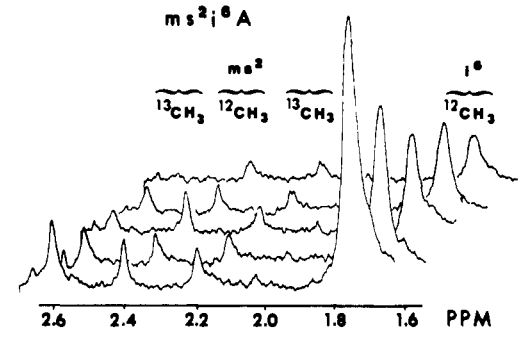

FIGURE 5: Proton spin-echo spectra of [^{13}C]methyl-enriched $tRNA^{Phe}$. In order to examine the carbon–proton scalar coupling and methyl proton relaxation (T_2) of ^{13}C-enriched tRNA, it was necessary to take ^1H NMR spectra of $tRNA^{Phe}$ and $tRNA^{Cys}$. The figure shows a set of spectra from a Hahn spin-echo experiment ($90°-\tau-180°-\tau$ pulse sequence) on $tRNA^{Phe}$. Five delays between 2 and 30 ms were used for this experiment. The ^{13}C split of the methyl protons of the ms group of ms^2i^6A is clearly seen even in samples without Mg^{2+}. Since the methyl groups of the isopentenyl group are not ^{13}C enriched, ^{13}C splitting of these methyl protons is not exhibited in the spectra.

°C (0.75–1.25 s) and again from 36 to 46 °C (1.25–1.62 s), before dramatically decreasing to 0.4 s at 65 °C. The T_1 value of m^7G in $tRNA^{Phe}$ increased from 0.80 s at 30 °C to 1.32 s at 36 °C, decreased to 1.10 s at 46 °C, and then decreased to 0.31 s at 65 °C.

Increases in T_1s of T and m^7G occurred at temperatures known to break the tertiary interactions responsible for the tRNA three-dimensional structure. T at position 54 and m^7G at position 46 are involved in tertiary structure and base-stacking interaction. It is quite possible that the increased T_1s of these methyl groups between 30 and 46 °C are caused by the larger hydrodynamic volume and thus slower tumbling of the molecule, after breakage of the tertiary bonds. With maintenance of most of the secondary-structure H bonds and base-stacking interactions at 46 °C in the presence of Mg^{2+}, motion of the bases contributes little to the T_1. However, at higher temperatures secondary-structure H bonds and stacking interactions dissolve, allowing motion of the bases to which the methyls are attached. This would be responsible for the decreased T_1 for all three methyl groups at the high temperatures. The methyl of ms^2i^6A located in the anticodon loop where base-stacking interactions predominate exhibited only a decrease in T_1, and that occurred after 46 °C. This base does not sample the breakage of tertiary interactions probed by T and m^7G.

In the absence of Mg^{2+}, the T_1s of the methyl groups of T and ms^2i^6A from $tRNA^{Cys}$ went through a maximum at a lower temperature. The T_1 of T increased from 0.95 s at 25 °C to 1.65 s at 30 °C before decreasing to 1.25 s at 36 °C. The T_1 of ms^2i^6A increased from 0.75 s at 25 °C to 1.1 s at 30 °C before retreating to 0.7 s at 36 °C.

The nuclear Overhauser enhancement (NOE) was measured for tRNAs specific for Phe, Tyr, and Cys in the absence of Mg^{2+} and for these plus $tRNA^{Ser}$ in the presence of the divalent ion (Table IIIB and Figure 4). NOE values for the methylthio groups of the first three tRNAs were quite comparable in the presence as well as in absence of Mg^{2+}, averaging 1.60 ± 0.1 s with Mg^{2+} and 1.51 ± 0.05 s without Mg^{2+}. NOE values for T in Phe, Cys, and Tyr tRNAs decreased upon addition of Mg^{2+}. With 10 mM $MgCl_2$, the NOEs for T's of $tRNA^{Phe}$ and $tRNA^{Tyr}$ were comparable (1.53 and 1.56), and those of $tRNA^{Cys}$ and $tRNA^{Ser}$ were lower and also similar to each other (1.28 and 1.30). It is interesting that these pairs are also distinct in the appearance of their spectra with regard to T in the absence of Mg^{2+} (Figure 1). For $tRNA^{Phe}$ and $tRNA^{Tyr}$ the T methyl is split into at least two peaks while for the Ser and Cys species T always gives a single resonance.

Tyr- and Ser-specific tRNA contain 2′-*O*-methyl substitutions on Gm-18 ($tRNA^{Tyr}$) and Gm-18 plus Cm-32 ($tRNA^{Ser}$). In spectra of $tRNA^{Ser}$ with 10 mM $MgCl_2$, the 2′-*O*-methyl signals appear as two resonances at 58.4 and 58.9 ppm. The downfield peak has an NOE of 1.45, comparable to most other tRNA methyls with Mg^{2+}. But the upfield resonance has an amazingly high NOE value of 2.3 (Table IIIB).

Line widths were determined for the methyl groups in $tRNA^{Phe}$, $tRNA^{Cys}$, $tRNA^{Tyr}$, and $tRNA^{Ser}$ in the presence of $MgCl_2$. Values for T were similar, between 10 and 14 Hz, whereas those for ms^2i^6A varied between 7 Hz for $tRNA^{Ser}$ and 14 Hz for $tRNA^{Cys}$ (Table IIIC).

^1H NMR Spectra of ^{13}C-Enriched tRNA. Proton NMR spectra of [^{13}C]methyl-enriched tRNA species exhibited the expected carbon-13 splitting of the methyl proton signals (Figure 5). The carbon–proton coupling constant for the methyl group of ms^2i^6A was 143 ± 1 Hz; for the methyl group of T, the value was 132 ± 1 Hz. With the addition of $MgCl_2$, the methyl proton signals for T and ms^2i^6A moved upfield, while the methyl proton signal for m^7G moved downfield. The direction of these changes in chemical shifts for the proton signals were analogous to that exhibited by the carbon signals from the same methyl groups. The magnitude of the change in chemical shift was smaller in the case of methyl proton signals (12–28 Hz) compared to that of the methyl carbon signals (8–75 Hz). A spin-echo experiment (Figure 5) with $tRNA^{Phe}$ demonstrated that the [^{12}C]methyl protons had a considerably longer T_2 (112 ± 11 ms) than the [^{13}C]methyl protons (47 ± 8 ms), reflecting additional dipolar relaxation due to the ^{13}C. Similar behavior was seen with $tRNA^{Cys}$.

Transfer RNA Methyl Group Dynamics. Given T_1 and NOE (and T_2) values for methyl groups, we can begin to learn about the motional dynamics of these methyl groups. We need to assume a relatively simple model for motion since our data is limited. As a first approximation, the bases are assumed to be stacked and to reorient with the whole tRNA, which in turn tumbles isotropically in solution. Methyl groups reorient by internal diffusion around the axis connecting them to their bases. Dipolar coupling to directly bonded hydrogens is the dominant source of relaxation. C–H bond distances were taken as 1.09 Å, and the tetrahedral bond angle was chosen. With this construct, we used the theory of Woessner (1962) to solve for τ_i, the internal correlation time for the methyl group, and τ_R, the overall correlation time. T_1 and NOE data were used for tRNAs in 10 mM $MgCl_2$ at 25 °C. These data and the

Table IV: Free Internal Diffusion of Methyls on tRNA

tRNA	methyl group	NOE $(1+\eta)$	$1/(NT_1)^a$ (s^{-1})	τ_i (ps)	τ_R (ns)
Phe	T	1.53	0.43	1.6	10
	ms^2 (i^6A)	1.69	0.36	2.0	14
	m^7G	1.43	0.35	1.0	12
Ser	T	1.30	0.29	0.4	13
	ms^2 (i^6A)	1.44	0.31	0.8	13
	Cm[b]	2.30	0.16	3.0	25
	Gm[b]	1.45	0.29	0.8	15
Cys	T	1.28	0.20	0.25	19
	ms^2 (i^6A)	1.66	0.16	0.8	30
Tyr	T	1.56	0.16	0.8	22
	ms^2 (i^6A)	1.44	0.26	0.8	16
	Gm[b]	1.59	0.14	0.6	32

[a] N is the number of directly bonded protons. [b] Cm and Gm are tentatively assigned to the high-field (58.36 ppm) and low-field (58.97 and 59.10 ppm) 2′-*O*-methyl signals of tRNAs for Ser and Tyr.

resulting correlation times are listed in Table IV.

Most internal correlation times lie within a factor of 2 of 1 ps. Overall τ_R values are fairly consistent for different groups in the same tRNA. Strictly speaking, the model would have them exactly the same. Different tRNA species appear to have significantly different τ_R values; $tRNA^{Phe}$ reorients most rapidly ($\tau_R \approx 12$ ns) while $tRNA^{Cys}$ is about 2 times slower. These tRNAs have the same molecular weight so that the difference in τ_R may actually reflect differences in flexibility of the structure. Other measurements of τ_R for tRNA under similar conditions have yielded values in the range of 16–30 ns, so the present analysis is in line with these (Schmidt et al., 1980; Komoroski & Allerhand, 1972; Patkowski & Chu, 1979).

One resonance has remarkable properties, the upfield 2′-*O*-methyl peak from methylated riboses of $tRNA^{Ser}$. With its very large NOE value (2.3) and long T_1 (2.04 s), it is out of line with the other peaks. However, these values might result from further motion about the ribose $C_{2'}$–O bond in addition to methyl rotation, a very reasonable sort of behavior. Even if the motion is restricted in amplitude, it can lead to increased NOEs and T_1 values (London & Avitable, 1978). Such extra internal motion should also contribute to the narrowing of the peak (longer T_2), but in fact, this resonance is actually broader than most (Table IIIC). It could be a composite of resonances or else be exchange broadened.

We were very interested to see if the methylthio group of ms^2i^6A showed evidence of significant motion around the Ade–S bond as well as the *S*-methyl linkage. In general the methylthio relaxation behavior for all tRNAs is similar to that of T and consistent with only limited amplitude excursions around the base–S bond, if any, on a fast time scale ($\tau_i \lesssim 10^{-7}$ s).

While more relaxation data at other NMR frequencies will provide greater detail on tRNA-modified base motion, it appears that fast rotational diffusion of methyl groups is the greatest contributor to relaxation from internal motion. Large-scale motion of the bases relative to the overall tRNA structure is precluded.

Registry No. T, 1463-10-1; ms^2i^6A, 20859-00-1; m^7G, 20244-86-4; Gm, 2140-71-8; Cm, 2140-72-9.

References

Agris, P. F. (1983) *The Modified Nucleosides of Transfer RNA: Volume II*, Liss, New York (in press).

Agris, P. F., & Schmidt, P. G. (1980) *Nucleic Acids Res. 8*, 2085–2091.

Agris, P. F., Koh, H., & Söll, D. (1973a) *Arch. Biochem. Biophys. 154*, 277–282.

Agris, P. F., Söll, D., & Seno, T. (1973b) *Biochemistry 12*, 4331–4337.

Agris, P. F., Powers, T., Söll, D., & Ruddle, F. (1974) *Cancer Biochem. Biophys. 1*, 69–77.

Agris, P. F., Tompson, J. G., Gehrke, C. W., Kuo, K. C., & Rice, R. H. (1980) *J. Chromatogr. 194*, 205–212.

Dirheimer, G., Keith, G., Sibler, A. P., & Martin, R. P. (1979) in *Transfer RNA: Structure, Properties and Recognition*, Cold Spring Harbor Laboratory, Cold Spring Harbor, NY.

Freeman, R., & Hill, H. D. W. (1971) *J. Chem. Phys. 54*, 3367–3377.

Jelinski, L. W., Sullivan, C. E., & Torchia, D. A. (1980) *J. Magn. Reson. 41*, 133–139.

Komoroski, R. A., & Allerhand, A. (1972) *Proc. Natl. Acad. Sci. U.S.A. 69*, 1804–1808.

London, R. E. (1980) in *Magnetic Resonance in Biology* (Cohen, J. S., Ed.) pp 1–69, Wiley, New York.

London, R. E., & Avitable, J. (1978) *J. Am. Chem. Soc. 100*, 7159–7165.

Patkowski, A., & Chu, B. (1979) *Biopolymers 18*, 2051–2072.

Schmidt, P. G., Tompson, J. G., & Agris, P. F. (1980) *Nucleic Acids Res. 8*, 643–656.

Seno, T., Agris, P. F., & Söll, D. (1974) *Biochim. Biophys. Acta 349*, 328–338.

Sprinzl, M., & Gauss, D. (1982) *Nucleic Acids Res. 10*, r1–r55.

Tompson, J. G., & Agris, P. F. (1979) *Nucleic Acids Res. 7*, 765–779.

Tompson, J. G., Hayashi, F., Paukstelis, J. V., Leoppky, R. N., & Agris, P. F. (1979) *Biochemistry 18*, 2079–2085.

Woessner, D. E. (1962) *J. Chem. Phys. 36*, 1–4.